

RESEARCH ARTICLE

Open Access



Electrochemical study of agarose hydrogels for natural convection on macroelectrodes and ultramicroelectrodes

Jihun Han^{1†}, Sukman Jang^{2†}, Byung-Kwon Kim^{3*} and Kyungsoon Park^{1*} 

Abstract

Electrochemical measurements using an agarose hydrogel as a solid electrolyte and ferrocyanide as a redox probe were conducted to analyze transport properties and natural convection effects. The mass transport properties and diffusion coefficients of ferrocyanide were studied using various macroelectrodes and ultramicroelectrodes via cyclic voltammetry. The experimental results confirmed that the mass transfer behavior in agarose was similar to that in solution. The good linearity of the square root of the scan-rate-dependent peak current demonstrated that diffusion is dominant during mass transfer in agarose hydrogel owing to a reduction in other mass transport effects (i.e., migration and convection). Furthermore, chronoamperometry (CA) was performed to estimate the effects of natural convection in the solution and agarose hydrogel. CA curves and plots of current as a function of the inverse square root of time yielded irregular and irreproducible responses in the solution for relatively long-term electrochemistry. However, in the agarose hydrogel, the CA response was more regular and reproducible for > 300 s because of reduced natural convection, based on the Cottrell's theory.

Keywords Agarose hydrogel, Natural convection, Mass transport properties, Long-term electrochemistry

Introduction

Hydrogels are promising materials for diverse applications, including energy storage and conversion (Feig et al. 2018; Lopez et al. 2018), drug delivery (Vashist et al. 2014; Dreiss 2020), biosensors (Khajouei et al. 2020; Kim and Shin 2021), and electrochemical devices (Wang et al. 2015, 2018), owing to their high electronic

conductivity (Zhu et al. 2015; Wu et al. 2013; Zhong et al. 2015), structural tunability (Zhao et al. 2017), and mass transport properties (Kim and Park 2022). Hydrogels are three-dimensional (3D) networks of hydrophilic polymer chains that can contain a large amount of water without dissolving (Lee and Mooney 2001). Hydrogel polymers can be classified into three categories based on their composition (Peppas et al. 2006): (1) synthetic polymers, (2) natural polymers, and (3) hybrid materials prepared from both synthetic and natural sources. Among natural hydrogels, agarose with a linear polysaccharide consisting of 1,3-linked β -D-galactopyranose and 1,4-linked 3,4-anhydro- α -L-galactopyranose as a repeating unit is commonly used because of its biocompatibility, nontoxicity, low cost, and good experimental properties (Fatin-Rouge et al. 2003; Hou et al. 2020).

Mass transfer (e.g., diffusion, migration, and convection), which is the movement of material from one location to an electrode surface, is crucial for

[†]Jihun Han and Sukman Jang have contributed equally to this work

*Correspondence:

Byung-Kwon Kim

kimb@ewha.ac.kr

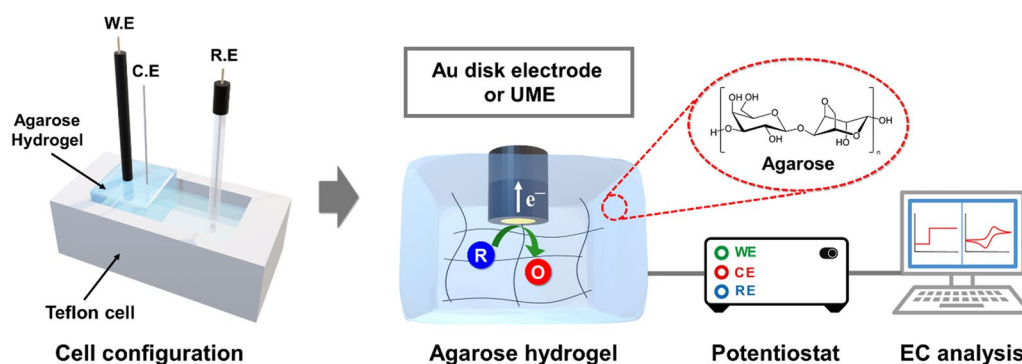
Kyungsoon Park

kspark895@jejunu.ac.kr

¹ Department of Chemistry and Cosmetics, Jeju National University, Jeju 690-756, Republic of Korea

² Department of Chemistry, Dankook University, 119 Dandaero, Cheonan 31116, Republic of Korea

³ Department of Chemistry and Nanoscience, Ewha Womans University, Seoul 03760, Republic of Korea



Scheme 1 Schematic of the electrode configuration for the electrochemical measurements

electrochemical reactions. Therefore, gaining insights into transport properties is essential for electrochemical applications using the solution phase and hydrogels. The mass transport behavior in polymeric hydrogels has rarely been reported. Recently, we examined the mass transport properties of redox molecules at the interface between an agarose hydrogel and a gold electrode and its slow-scan voltammetry without natural convection (Kim and Park 2022). The minimization of natural convection and migration using hydrogels is beneficial for long-term electrolysis to obtain good reproducibility and ensure compliance with fundamental theories (e.g., Randles-Sevcik, Cottrell, and Shoup and Szabo equations) (Kim et al. 2020; Tsierkezos 2007; Foster et al. 1989; Shoup and Szabo 1982). The controlling nanoparticles such as size, morphology, and crystal structures are very important features in electrochemical deposition. Therefore, hydrogel media is expected to be a good template for the electrodeposition of metal nanoparticles due to the reduced irregular transport (e.g., natural convection) of solute.

An ultramicroelectrode (UME) is defined as an electrode with at least one of the critical dimensions (e.g., disk electrode radius or width and length of the band electrode) smaller than $\sim 25 \mu\text{m}$ (Faulkner and Bard 2000). Since its introduction in the late 1970s, UMEs have been widely used for electrochemical analysis because their unique behavior differs from that of conventional macroelectrodes. The advantageous properties of UMEs are as follows.

1. UMEs exhibit higher signal-to-noise ratios, lower detection limits, and enhanced sensitivity for electrochemical analysis than macroelectrodes. The noise signal is proportional to the electroactive area of the electrode, whereas the Faradaic response related to the redox reaction of the analyte is proportional to the total electrode area, including the active and inactive areas (Tomcik 2013).

2. The ohmic drop or iR drop caused by the solution resistance between the working and reference electrodes is negligible because of the low current flow at the UME (typically on a nA to pA scale) (Walsh et al. 2010). These properties render them as particularly versatile tools for analytical purposes, including electrochemical measurements in solutions with low electrolyte concentrations, organic solvents, and solid or gas phases (Heinze 1993).
3. UMEs can operate in the early transient state because of the low cell time constant (RC) and in the steady-state regime owing to enhanced mass transfer properties. Consequently, UMEs are particularly suited for the study of rapid homogeneous or heterogeneous reactions (Zoski 2002).

Previous studies using UMEs have been generally performed in the solution phase, and electrochemical phenomena were rarely examined at the hydrogel/UME interface.

Herein, the mass transfer properties of agarose hydrogels (particularly convection) were examined on macroelectrodes and a UME. Cyclic voltammetry (CV) and chronoamperometry (CA) were performed under macro-disk-electrode and UME conditions, and the diffusion coefficient (D) of the redox species was calculated using the measured current values. Based on the results, the concentration of agarose hydrogel optimal for each electrode is presented. The homemade cell and electrode setup are shown in Scheme 1.

Experimental

Materials

Potassium chloride (99.9%), agarose powder, and potassium hexacyanoferrate(II) trihydrate (99.9%) were purchased from Sigma-Aldrich (St. Louis, MO, USA). An Au disk electrode (1.6 mm diameter) was obtained from BAS Inc. Prior to the experiment, the Au disk electrode was

polished using MicroPolish alumina (0.3 and 0.05 μm) powders and a polishing micro-cloth pad obtained from Buehler. Au (99.99%) microwires (25 μm diameter) were purchased from Goodfellow (Devon, PA, USA). All chemicals and reagents used herein were of reagent grade. Deionized water ($>18\text{ M}\Omega\text{ cm}$) was obtained using a Millipore Milli-Q purification system.

Preparation of the agarose hydrogel for electrochemistry

Various concentrations of aqueous agarose (9.1, 4.8, 3.2, and 2.4 wt% agarose) were prepared in heat-resistant containers with caps. The containers with agarose solution were placed in a water bath at 90 $^{\circ}\text{C}$ for 1 h until the agarose was completely dissolved. Air bubbles, which can disrupt solute transport in the gel, were removed using a vacuum pump. The prepared melted agarose solution was poured into a glass mold. Before the agarose solidified, the Au disk electrode was inserted into the agarose solution, fixed vertically with a clamp, and slowly cooled in a controlled humidity chamber. After gelation, agarose hydrogel exhibited a rigid and insoluble polymer network and was reusable. For electrochemical measurements, the Au disk electrode-equipped agarose hydrogels were immersed in an aqueous solution containing redox molecules and supporting electrolytes for 24 h to achieve complete equilibrium.

Fabrication method of the UME

The Au UME was fabricated using the following process (Lee et al. 2021): The Au microwire was washed several times with ethanol and distilled water. The cleaned Au microwire was subsequently placed on one side of the capillary and sealed. A metal wire was inserted into the opposite hole and bonded to an Au microwire using silver paste. The capillary was then polished so that the Au microwire was exposed to the capillary surface. The Au microwire was polished until a mirror surface was obtained, and the electrode surface area was calibrated using a ferrocene–methanol solution.

Electrochemical measurements

The electrochemical cell consisted of a conventional three-electrode setup with an Au disk electrode and UME as the working electrode, Pt wire as the counter electrode, and Ag/AgCl as the reference electrode. Both the working and counter electrodes were positioned inside the agarose hydrogel. The electrochemical experiments were performed using a CHI 601e potentiostat (CH Instruments, Austin, TX, USA) in a Faraday cage. CA was performed to examine the effect of natural convection by applying 0.3 V (vs. Ag/AgCl) to the working electrode.

Results and discussion

To analyze the mass transport properties of the solute in solution and at various concentrations of hydrogel, $\text{Fe}(\text{CN})_6^{4-}$ was selected as an electrochemical redox probe that performs one-electron transfer and exhibits good electrochemical reversibility. Figure 1a shows the CV curves of $\text{Fe}(\text{CN})_6^{4-}$ on the Au disk electrode in solution as a function of scan rate. In solution, the measured peak-to-peak separation (ΔE) is $\sim 63\text{ mV}$, which is similar to the theoretical ΔE value of a one-electron reversible system (57 mV at 25 $^{\circ}\text{C}$) (Faulkner and Bard 2000). Additionally, both the anodic and cathodic peak currents increase with increasing scan rate, and a linear relationship between the square root of the scan rate and peak current is shown in Fig. 1b. This linearity demonstrates that mass transport is mainly controlled by diffusion in the solution phase (Amatore et al. 2001).

The agarose gel possesses a porous structure with a wide distribution of pore sizes ranging from 1 to 900 nm depending on the gel concentration (Maaloum et al. 1998). The transport of redox probes through gel channels/pores to the electrode surface is crucial for their electrochemistry. As the concentration of agarose increases from 2.4 to 9.1 wt%, both the anodic and cathodic peak currents (I_p) decrease compared with those of the solution phase. Additionally, with increasing agarose concentration, the voltammograms are slightly anodically shifted to approximately 10–12 mV. This anodic shift implies a higher degree of interaction and stabilization between the charged $\text{Fe}(\text{CN})_6^{4-}$ molecule and hydrophilic moieties of the agarose polymer backbone. From these results, the redox probe is sufficiently small to move freely in the hydrogel networks at the gel composition tested herein (Kanievska et al. 2020). In addition, from the plot of scan rate (ν) vs. I_p (see Additional file 1: Fig. S1), it was confirmed that redox species in solution and agarose hydrogel were transported to the electrode by freely diffusion without any hindering of adsorption.

To confirm the diffusion properties of the redox molecules, the D of $\text{Fe}(\text{CN})_6^{4-}$ in the agarose gel was calculated using the Randles–Sevcik equation at room temperature (Faulkner and Bard 2000).

$$I_p = (2.69 \times 10^5) n^{3/2} A D^{1/2} C \nu^{1/2} \quad (1)$$

where I_p is the net peak current (A); n is the number of electrons transferred in the redox event; A is the electrode area (cm^2); D is the redox diffusion coefficient (cm^2/s); C is the bulk redox concentration (mol/cm^3); and ν is the scan rate (V/s). The D of $\text{Fe}(\text{CN})_6^{4-}$ in the solution phase determined using Eq. (1) was $6.34 \times 10^{-6}\text{ cm}^2/\text{s}$. Based on this value, the D values of $\text{Fe}(\text{CN})_6^{4-}$ are

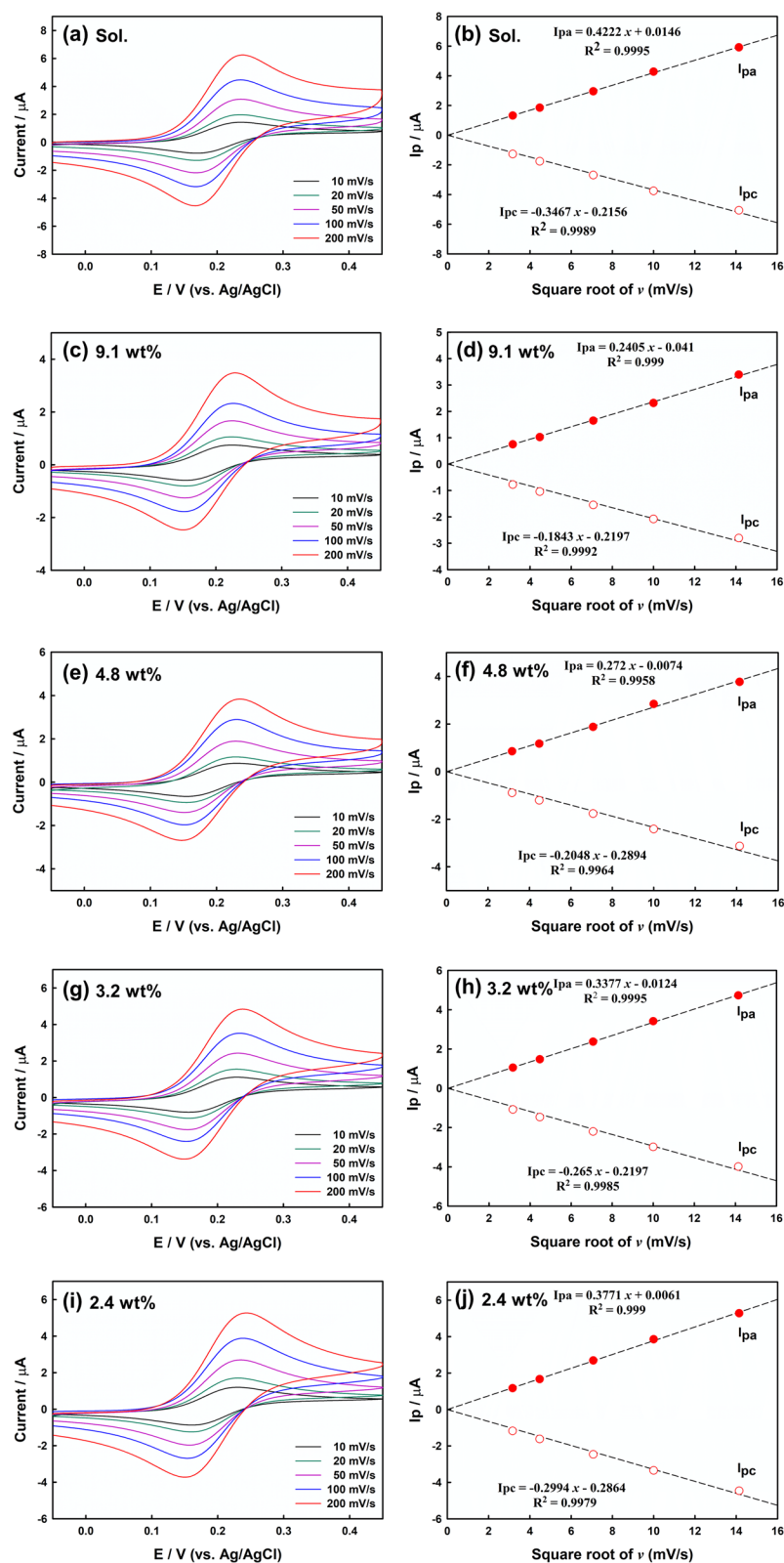


Fig. 1 CV curves of the Au disk electrode in aqueous solution and at various concentrations of agarose hydrogels, and plots of the peak current (I_p) as a function of the square root of the scan rate **b, d, f, h, i** containing 1 mM $\text{Fe}(\text{CN})_6^{4-}$ and 0.1 M KCl. **a** and **b** In solution phase; **c** and **d** 9.1 wt% agarose; **e** and **f** 4.8 wt% agarose; **g** and **h** 3.2 wt% agarose; and **i** and **j** 2.4 wt% agarose.

compared at various agarose concentrations, as shown in Fig. 2. The D values in agarose are approximately the same order of magnitude as those in the solution, but the mass transport properties deteriorate with increasing agarose concentrations. These results possibly originate from the hindered permeability of the solute in agarose, which is assumed to be caused by steric hindrance and interactions between the solute and agarose polymer network (Ciszkowska and Guillaume 1999; Crumbliss et al. 1992). However, at 2.4 wt% agarose, the D of the solute is $5.15 \times 10^{-6} \text{ cm}^2/\text{s}$ (Fig. 2a). This slight difference in the D value can be explained by the good permeability of the solute through the water portion of the agarose gel, even in the polymer. At agarose concentrations of <2.4 wt%, transport through the hydrogel for electrochemistry is difficult, since agarose concentrations below 2.4 wt% are considered too dilute and hard to form a rigid polymer structure.

Figure 2b shows the dependence of I_p on $v^{1/2}$ in solution and at various agarose concentrations. I_p increases with increasing scan rate, and a linear relationship between I_p and $v^{1/2}$ is observed. Additionally, the slope related to the solute D decreases with increasing agarose concentration due to the increased steric hindrance between solute and agarose polymer fibers. The linearity of this process generally indicates that the redox molecule mass transfer is mainly governed by a diffusion-controlled process. Therefore, regardless of the agarose hydrogel concentration, diffusion is a dominant factor in mass transfer.

Mass transfer in agarose hydrogels in the UME was also examined. A UME is an electrode with a diameter of several tens of micrometers or less and is a good electrode for observing electrochemical phenomena in a small area. For UMEs, because mass transfer follows hemispherical

diffusion, a current decrease does not occur even at potentials exceeding the E_p value, as opposed to the trend in macroelectrodes. Therefore, it is a more convenient method for calculating the D values of the redox species. As shown in Fig. 3a, it is confirmed that a steady-state current (I_{ss}) is achieved at various agarose hydrogel concentrations. The I_{ss} of the UME can be described using the following equation: (Faulkner and Bard 2000; Kim et al. 2021)

$$I_{ss} = 4nFDcr \quad (2)$$

where r denotes the UME radius. Using Eq. (2), the D of $\text{Fe}(\text{CN})_6^{4-}$ can be calculated. The D values of $\text{Fe}(\text{CN})_6^{4-}$ calculated at various agarose hydrogel concentrations are shown in Fig. 3b. In the 2.4 and 3.2 wt% agarose hydrogels, the D of $\text{Fe}(\text{CN})_6^{4-}$ is similar to the value measured at the macroelectrode. However, the D deviates from linearity under high-concentration agarose hydrogel conditions (4.8 and 9.1 wt%). This can be attributed to the inhomogeneity of the part of the agarose hydrogel in contact with the UME inside the gel. Agarose hydrogel homogeneity generally decreases at high agarose concentrations. The surface area of the UME is 0.000491 mm^2 , which is very small compared to that of the macroelectrode ($\sim 2.01 \text{ mm}^2$; $1/4096$). Therefore, the current of the UME is affected by the inhomogeneity of the high-concentration agarose hydrogel, and the D of $\text{Fe}(\text{CN})_6^{4-}$ must be calculated differently. Therefore, agarose hydrogels with agarose concentration exceeding 4.8 wt% are not recommended for use in conjunction with UMEs.

CA was conducted using a macroelectrode and UME with various agarose hydrogel concentrations. CA is a potential step technique that is essential for the analysis of adsorption, chemical reactions, and diffusion

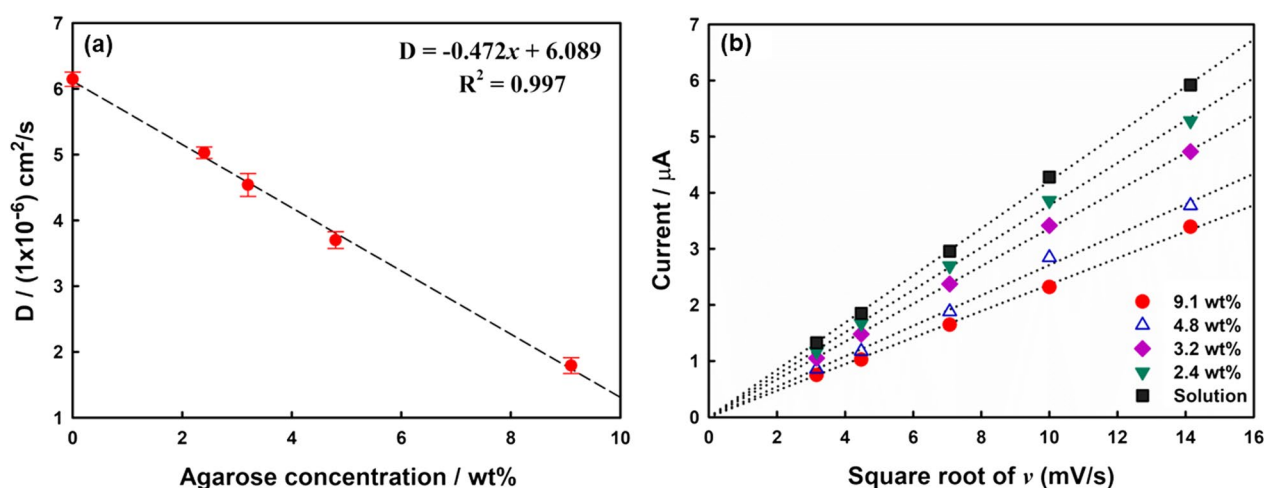


Fig. 2 a D of $\text{Fe}(\text{CN})_6^{4-}$ as a function of the agarose concentration in the gel. Error bars are obtained based on three independent measurements. b Plots of the anodic peak current as a function of $v^{1/2}$ at various agarose concentrations

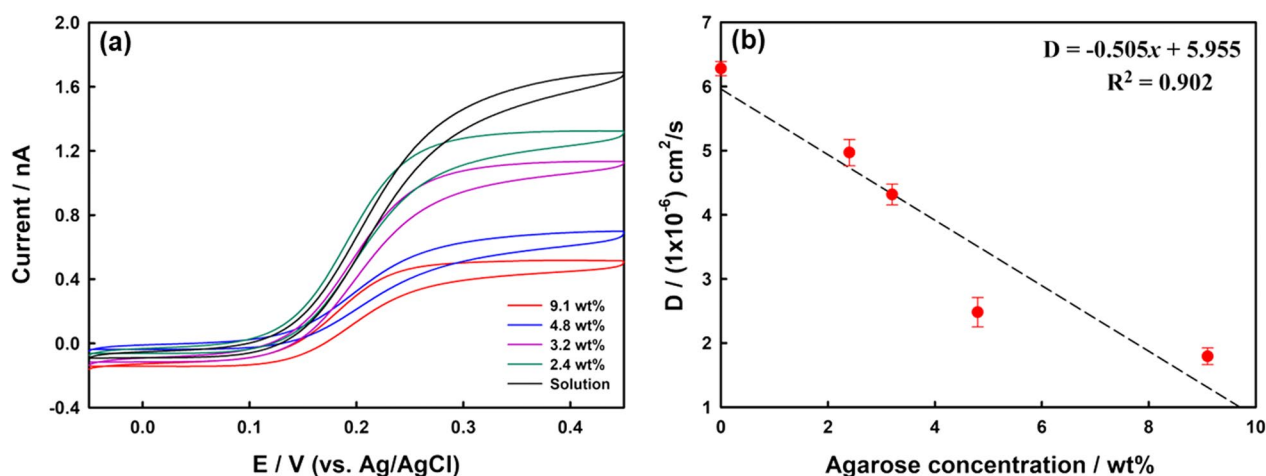


Fig. 3 **a** CV curves of the Au UME (25 μm diameter) in the agarose hydrogel depending on the agarose concentration (colored line) and in solution (black line) containing 0.5 mM $\text{Fe}(\text{CN})_6^{4-}$ and 0.1 M KCl. Scan rate: 10 mV/s. **b** D of $\text{Fe}(\text{CN})_6^{4-}$ as a function of the agarose concentration. Error bars are obtained based on three independent measurements

processes. However, long-term CA frequently provides irregular and irreproducible results owing to unexpected natural convection, causing deviations from theoretical results. The CA for test durations > 20 s may include convective hindrance, and that for > 300 s is no longer controlled by diffusion (Faulkner and Bard 2000). The natural convection that occurs from the density gradient (Gao et al. 1995), thermal convection (Novev et al. 2016), and mechanical vibration (Amatore et al. 2001) can disrupt the diffusion layer and generally produces a larger current than those predicted by the Cottrell equation.

Figure 4a shows the CA curves of $\text{Fe}(\text{CN})_6^{4-}$ in solution (black line) and in various agarose concentrations

(colored lines). The current curves obtained in the agarose hydrogel represent smooth and reproducible current decay, but the current in the solution phase is irreproducible and larger than those in the agarose hydrogel at > 30 s. Figure 4b shows the plots of I vs. $t^{-1/2}$ of Fig. 4a. In the agarose hydrogel, regardless of the agarose concentration, a good linear relationship between the current and $t^{-1/2}$ is established over a long time (> 100 s), demonstrating a diffusion-controlled process for the electrochemical reaction and the effective prevention of natural convection. However, the steady-state current in solution (black line) shows deviation from linearity, and the irregular curve is assumed to arise from natural convection

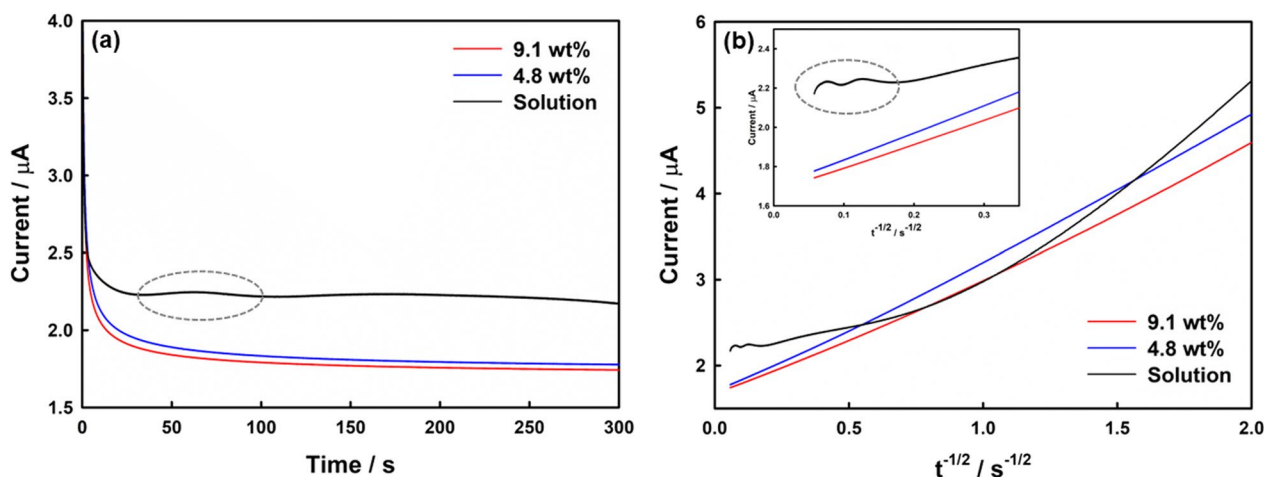


Fig. 4 **a** CA curves of 1 mM $\text{Fe}(\text{CN})_6^{4-}$ and 0.1 M KCl in various agarose hydrogel concentrations (colored lines) and in solution (black line) at an applied potential of 0.3 V using a Au disk electrode. **b** Plots of current as a function of the $t^{-1/2}$ of (a) and highlighted long-term domain (inset). The gray dotted circle showed the current fluctuations due to the natural convection

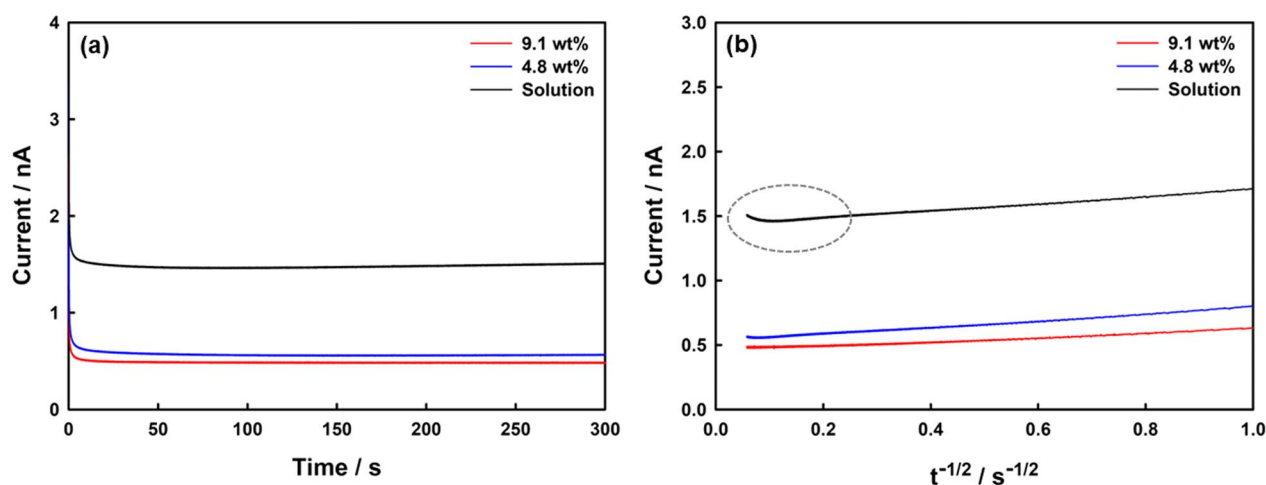


Fig. 5 **a** CA curves of 0.5 mM $\text{Fe}(\text{CN})_6^{4-}$ and 0.1 M KCl in various agarose hydrogel concentrations (colored lines) and in solution (black line) at 0.3 V, which is applied to an Au UME. **b** Plots of current as a function of $t^{-1/2}$ of (a). The gray dotted circle showed the current fluctuations due to the natural convection

effects (Labille et al. 2007). Natural convection is considered to play a dominant role at this time scale. These CA results indicate that natural convection can be successfully reduced using the agarose hydrogel, even during long-term electrolysis.

The CA measurement results for 0.5 mM $\text{Fe}(\text{CN})_6^{4-}$ obtained using the UME are shown in Fig. 5a. Very low currents (e.g., nA to pA scale) are generally measured in a UME. Because the nA level is significantly affected by background current noise, the electrochemical cell is generally placed in a Faraday cage when using a UME for electrochemical measurements. Faraday cages reduce background current noise and unexpected vibration or convection. As shown with the black line in Fig. 5a, the current fluctuations measured in solution are reduced compared to the macroelectrode measurements.

However, small fluctuations are observed in the long-time region (>100 s). The use of agarose hydrogels can further suppress these fluctuations. Figure 5b provides further insights into this phenomenon. In the long-time region, the current fluctuations are hardly observed in the agarose hydrogel (red and blue lines in Fig. 5b). Therefore, agarose hydrogels present a promising option for minimizing unexpected convection, even under UME conditions.

Conclusions

This study confirmed the solute mass transport properties within an agarose hydrogel using a macroelectrode and UME. CV curves obtained in various agarose concentrations demonstrated diffusion-controlled behavior in the hydrogels, despite the reduced diffusional properties compared to the solution phase owing to steric

hindrance between the solute and agarose polymer network. The electroactive molecule was sufficiently small to freely penetrate the hydrogel pores at the hydrogel compositions tested herein. Additionally, the CA of the agarose hydrogel showed a more regular and reproducible current for >300 s based on the Cottrell's theory, owing to reduced natural convection. The results presented herein suggest that hydrogels as solid electrolytes are ideal mediums with negligible interference for long-term CA and slow-scan voltammetry (e.g., migration or convection).

Supplementary Information

The online version contains supplementary material available at <https://doi.org/10.1186/s40543-023-00375-4>.

Additional file 1. Figure S1. The plots of the peak current (I_p) vs. scan rate (v) under the same conditions as in Fig. 1. (a) in solution; (b) 9.1 wt% agarose; (c) 4.8 wt% agarose; (d) 3.2 wt% agarose; and (e) 2.4 wt% agarose.

Acknowledgements

We highly appreciate the editor to improve our manuscript by constructive comments.

Author contributions

JH and SJ conceptualized and performed experiments, and BKK and KP directed the research and data analysis. All authors have read and agree to the published version of the manuscript. All authors read and approved the final manuscript.

Funding

K.P. acknowledges support from the Basic Science Research Program of the Research Institute for Basic Sciences (RIBS) of Jeju National University through the National Research Foundation of Korea (NRF) funded by the Ministry of Education (2019R1A6A1A10072987). This research was also supported by the Basic Science Research Program through the National Research Foundation of Korea (NRF) funded by the Ministry of Education (NRF-2022R111A3072996). B.K. was supported by the Basic Science Research Program through the

National Research Foundation of Korea (NRF) funded by the Ministry of Education (2021R1A6A1A10039823), the National Research Foundation (NRF) of Korea, which is funded by the Ministry of Science and ICT (NRF-2021R1A2C4002069), and the Korea Basic Science Institute (National Research Facilities and Equipment Center) grant funded by the Ministry of Education (2020R 1A 6C 101B194).

Availability of data and materials

Not applicable.

Declarations

Competing interests

The authors declare that they have no competing interests.

Received: 1 November 2022 Accepted: 26 January 2023

Published online: 08 February 2023

References

- Amatore C, Szunerits S, Thouin L, Warkocz JS. The real meaning of Nernst's steady diffusion layer concept under non-forced hydrodynamic conditions. A simple model based on Levich's seminal view of convection. *J Electroanal Chem*. 2001;500:62–70. <https://doi.org/10.1038/s41467-018-05222-4>.
- Ciszkowska M, Guillaume MD. Transport of ions and molecules in biopolymeric gels: electroanalytical studies. *J Phys Chem A*. 1999;103:607–13. <https://doi.org/10.1021/jp983389+>.
- Crumbless AL, Ferine SC, Edwards AK, Rillema DP. Characterization of carrageenan hydrogel electrode coatings with immobilized cationic metal complex redox couples. *J Phys Chem*. 1992;96:1388–94. <https://doi.org/10.1021/j100182a067>.
- Dreiss CA. Hydrogel design strategies for drug delivery. *Curr Opin Colloid Interface Sci*. 2020;20(48):1–17. <https://doi.org/10.1016/j.cocis.2020.02.001>.
- Fatin-Rouge N, Milon A, Buffle J. Diffusion and partitioning of solutes in agarose hydrogels: the relative influence of electrostatic and specific interactions. *J Phys Chem B*. 2003;2003(107):12126–37. <https://doi.org/10.1021/jp0303164>.
- Faulkner LR, Bard AJ. *Electrochemical methods fundamentals and applications*. 2nd ed. London: Wiley; 2000.
- Feig VR, Tran H, Lee M, Bao Z. Mechanically tunable conductive interpenetrating network hydrogels that mimic the elastic moduli of biological tissue. *Nat Commun*. 2018;9(1):2740. <https://doi.org/10.1038/s41467-018-05222-4>.
- Foster RJ, Kelly AJ, Vos JG. The effect of supporting electrolyte and temperature on the rate of charge propagation through thin films of [Os(bipy)₂PVP10Cl]Cl coated on stationary electrodes. *J Electroanal Chem*. 1989;270:365–79. [https://doi.org/10.1016/0022-0728\(89\)85049-1](https://doi.org/10.1016/0022-0728(89)85049-1).
- Gao X, Lee J, White HS. Natural convection at microelectrodes. *Anal Chem*. 1995;67:1541–5. <https://doi.org/10.1021/ac00105a011>.
- Heinze J. Ultramicroelectrodes in electrochemistry. *Angew Chem Int Ed Engl*. 1993;32:1268–88. <https://doi.org/10.1002/anie.199312681>.
- Hou M, Liu W, Zhang L, Zhang L, Xu Z, Cao Y, Kang Y, Xue P. Responsive agarose hydrogel incorporated with natural humic acid and MnO₂ nanoparticles for effective relief of tumor hypoxia and enhanced photo-induced tumor therapy. *Biomater Sci*. 2020;8(1):353–69. <https://doi.org/10.1039/c9bm01472a>.
- Kaniewska K, Bączal P, Sawicka M, Stojek Z, Karbarz M. Nanocomposite hydrogel coatings: formation of metal nanostructures by electrodeposition through thermoresponsive hydrogel layer. *Electrochim Acta*. 2020;363:137243. <https://doi.org/10.1016/j.electacta.2020.137243>.
- Khajouei S, Ravan H, Ebrahimi A. DNA hydrogel-empowered biosensing. *Adv Colloid Interface Sci*. 2020;275:102060. <https://doi.org/10.1016/j.cis.2019.102060>.
- Kim BK, Park K. Mass transport properties and influence of natural convection for voltammetry at the agarose hydrogel interface. *J Electrochem Sci and Technol*. 2022;13(3):347–53. <https://doi.org/10.33961/jecst.2022.00129>.
- Kim SJ, Shin W. Glucose diffusion limiting membrane based on polyethyleneimine (PEI) hydrogel for the stabilization of glucose sensor. *J Electrochem Sci and Technol*. 2021;12(2):225–9. <https://doi.org/10.33961/jecst.2020.01487>.
- Kim T, Choi W, Shin HC, Choi JY, Kim JM, Park MS, Yoon WS. Applications of voltammetry in lithium ion battery research. *J Electrochem Sci and Technol*. 2020;11(1):14–25. <https://doi.org/10.33961/jecst.2019.00619>.
- Kim HY, Lee J, Song S, Kang I, Kim SY, Kim BK. Simple method to analyze the molecular weight of polymers using cyclic voltammetry. *Sens Actuators B Chem*. 2021;330:129305. <https://doi.org/10.1016/j.snb.2020.129305>.
- Labille J, Rouge NF, Buffle J. Local and average diffusion of nanosolutes in agarose gel: the effect of the gel/solution interface structure. *Langmuir*. 2007;23:2083–90. <https://doi.org/10.1021/la0611155>.
- Lee KY, Mooney DJ. Hydrogels for tissue engineering. *Chem Rev*. 2001;101:1869–80. <https://doi.org/10.1021/cr000108x>.
- Lee J, Lee J, Song S, Kim BK. Single microcystis detection through electrochemical collision events on ultramicroelectrodes. *Bull Korean Chem Soc*. 2021;42(5):818–23. <https://doi.org/10.1002/bkcs.12237>.
- Lopez J, Sun Y, Mackanic DG, Lee M, Foudeh AM, Song MS, Cui Y, Bao Z. A dual-crosslinking design for resilient lithium-ion conductors. *Adv Mater*. 2018;30(43):e1804142. <https://doi.org/10.1002/adma.201804142>.
- Maaloum M, Pernodet N, Tinland B. Agarose gel structure using atomic force microscopy: gel concentration and ionic strength effects. *Electrophoresis*. 1998;19:1606–10. <https://doi.org/10.1002/elps.1150191015>.
- Novev JK, Eloul S, Compton RG. Influence of reaction-induced thermal convection on the electrical currents measured in chronoamperometry and cyclic voltammetry. *J Phys Chem C*. 2016;120(25):13549–62. <https://doi.org/10.1021/acs.jpcc.6b03413>.
- Peppas NA, Hilt JZ, Khademhosseini A, Langer R. Hydrogels in biology and medicine: from molecular principles to bionanotechnology. *Adv Mater*. 2006;18(11):1345–60. <https://doi.org/10.1002/adma.200501612>.
- Shoup D, Szabo A. Chronoamperometric current at finite disk electrodes. *J Electroanal Chem*. 1982;140:237–45. [https://doi.org/10.1016/0022-0728\(82\)85171-1](https://doi.org/10.1016/0022-0728(82)85171-1).
- Tomcik P. Microelectrode arrays with overlapped diffusion layers as electroanalytical detectors: theory and basic applications. *Sensors (Basel)*. 2013;13(10):13659–84. <https://doi.org/10.3390/s131013659>.
- Tsierkezos NG. Cyclic voltammetric studies of ferrocene in nonaqueous solvents in the temperature range from 248.15 to 298.15 K. *J Solution Chem*. 2007;36(3):289–302. <https://doi.org/10.1007/s10953-006-9119-9>.
- Vashist A, Vashist A, Gupta YK, Ahmad S. Recent advances in hydrogel based drug delivery systems for the human body. *J Mater Chem B*. 2014;2(2):147–66. <https://doi.org/10.1039/c3tb21016b>.
- Walsh DA, Lovelock KR, Licence P. Ultramicroelectrode voltammetry and scanning electrochemical microscopy in room-temperature ionic liquid electrolytes. *Chem Soc Rev*. 2010;39(11):4185–94. <https://doi.org/10.1039/b822846a>.
- Wang Y, Shi Y, Pan L, Ding Y, Zhao Y, Li Y, Shi Y, Yu G. Dopant-enabled supramolecular approach for controlled synthesis of nanostructured conductive polymer hydrogels. *Nano Lett*. 2015;15(11):7736–41. <https://doi.org/10.1021/acs.nanolett.5b03891>.
- Wang Z, Li H, Tang Z, Liu Z, Ruan Z, Ma L, Yang Q, Wang D, Zhi C. Hydrogel electrolytes for flexible aqueous energy storage devices. *Adv Funct Mater*. 2018;28(48):1804560. <https://doi.org/10.1002/adfm.201804560>.
- Wu H, Wang X, Jiang L, Wu C, Zhao Q, Liu X, Hu BA, Yi L. The effects of electrolyte on the supercapacitive performance of activated calcium carbide-derived carbon. *J Power Sources*. 2013;226:202–9. <https://doi.org/10.1016/j.jpowsour.2012.11.014>.
- Zhao F, Shi Y, Pan L, Yu G. Multifunctional nanostructured conductive polymer gels: synthesis, properties, and applications. *Acc Chem Res*. 2017;50(7):1734–43. <https://doi.org/10.1021/acs.accounts.7b00191>.
- Zhong C, Deng Y, Hu W, Qiao J, Zhang L, Zhang J. A review of electrolyte materials and compositions for electrochemical supercapacitors. *Chem Soc Rev*. 2015;44(21):7484–539. <https://doi.org/10.1039/c5cs00303b>.
- Zhu J, Xu Y, Wang J, Lin J, Sun X, Mao S. The effect of various electrolyte cations on electrochemical performance of polypyrrole/RGO based supercapacitors. *Phys Chem Chem Phys*. 2015;17(43):28666–73. <https://doi.org/10.1039/c5cp04080a>.
- Zoski CG. Ultramicroelectrodes: design, fabrication, and characterization. *Electroanalysis*. 2002;14:1041–51. [https://doi.org/10.1002/1521-4109\(200208\)14:15/16%3c1041::AID-ELAN1041%3e3.0.CO;2-8](https://doi.org/10.1002/1521-4109(200208)14:15/16%3c1041::AID-ELAN1041%3e3.0.CO;2-8).

Publisher's Note

Springer Nature remains neutral with regard to jurisdictional claims in published maps and institutional affiliations.